

Shock-Wave Consolidation of Rapidly Solidified Superalloy Powders

Marc A. Meyers and B. Bhushan Gupta
New Mexico Institute of Mining and Technology
Socorro, New Mexico

Lawrence E. Murr
Oregon Graduate Center
Beaverton, Oregon

Shock-Wave Consolidation of Rapidly Solidified Superalloy Powders

Marc A. Meyers and B. Bhushan Gupta
New Mexico Institute of Mining and Technology
Socorro, New Mexico

Lawrence E. Murr
Oregon Graduate Center
Beaverton, Oregon

SUMMARY

The feasibility of consolidating rapidly solidified MAR M-200 powders by explosive means is demonstrated. MAR M-200 powders produced by the rapid solidification rate (RSR) technique and exhibiting a microdendritic structure were consolidated in an axisymmetric set-up, consisting of a steel pipe (in which the powder was placed) surrounded by explosives. The converging shock waves produced full densification, after optimization of the process parameters. The microindentation hardness showed a dramatic increase: 357 HV in the as-received condition, to 700 HV in the shock-consolidated condition. The substructure was analyzed by TEM, and two distinct regions were identified. The center of the particles exhibited planar arrays of dislocations, stacking-faults, and twin faults characteristic of shock-loaded superalloys, while the melted and re-solidified interfacial layers consisted of a microcrystalline structure with homogeneous composition.

INTRODUCTION

Rapid solidification processing is an emerging technology of great potential, as evidenced by the two recent conferences devoted to the subject.^{1,2} Rapidly solidified powders can be made by a number of techniques:³ gas atomization, vacuum atomization, water atomization, ultrasonic atomization, electrostatic atomization, the rotating electrode process, and the rapid solidification rate process (RSR). RSR has been developed by Pratt and Whitney and yields cooling rates of 10^6 K/s for particles of 100 μm or less. These ultrahigh quenching rates minimize chemical segregation and the formation of massive phases.³ An added advantage is that the solubility of alloying elements is greatly increased.

Some of the methods that can be used to consolidate the powders have been traditionally used in powder metallurgy. However, the unique properties of the powders and the intended applications are such that new consolidation methods are being envisaged. Hot isostatic pressing, hot extrusion, hot isostatic pressing combined with isothermal forging, and dynamic compaction are the techniques offering the greatest potential.^{3,4} Of particular interest is dynamic compaction, since it would not require a post-deformation sintering stage that could degrade the unique properties of the powders. This paper describes the results obtained using such a technique.

Dynamic (or perhaps, more appropriately, shock-wave) compaction has been known and investigated for the past 20 years. Pearson⁵ was the first to use explosives to successfully consolidate titanium and iron filings. It seems that the Soviet research effort—particularly at the Powder Metallurgy Research Institute,^{6,7} in Minsk and at the Institute of Hydrodynamics,⁸ in Novosibirsk—has been much more intense than any U.S. counterpart. The process is described by Clyens and Johnson⁹ and Lennon et al.¹⁰

The essential feature of shock-wave compaction is the passage of a shock wave through the powder. This shock

wave takes a unique configuration due to the stress state established at the external layers of the particles, as will be explained later. The shock wave can be generated by either detonation of an explosive in direct contact with the system containing the powder or by impact of a high-velocity projectile against it. Raybould¹¹⁻¹³ successfully consolidated non-equilibrium alloys and AISI 304 L stainless steel using a specially constructed compressed-air gun driving a projectile. He reported very significant hardness increases and interparticle melting as an important part of the bonding and consolidation process. However, the size of these compacts is limited by the gun bore diameter, and scale-up requires great capital investment. Explosives provide an alternative means of producing such shock waves.

CHARACTERIZATION OF THE POWDER MAR M-200

MAR M-200 is a heat-resistant alloy used for jet turbine blades and vanes operating in the temperature range of 760-1100°C. Its major constituent elements are nickel (60%) and, in decreasing order, zirconium, cobalt, chromium, aluminum, and titanium. The RSR process is described by Hollday et al.¹⁴ To determine the particle size range, a two-stage sieve analysis was performed using U.S. standard sieve series. Table I shows the weight distribution of the various sizes. The majority of particles have diameters between 37 and 74 μm . A large percentage of the particles was found to be spherical, while a minority was elliptical or peanut-shaped. Figure 1a shows their general morphology. No flakes or angular contours were observed in these particles. In Figure 1b, which is a magnified view of a spherical particle, the surface texture, due to the dendritic solidification process, can be seen. This dendritic structure can be more clearly identified by increasing the magnification by a factor of ten (Figure 1c).

Upon polishing and etching after being mounted in an epoxy mount, the internal structure was revealed, as shown

TABLE I
Sieve Analysis of MAR M-200 Powder
(Feed size: 250 gram-force; Sieving time: 20 min)

U.S. Number (Mesh)	Opening (μm)	Yield Fraction (% wt)
>100	149	0
100-120	125	0
120-140	105	0.2
140-170	88	8.8
170-200	74	8.0
200-270	53	36.9
270-325	44	26.0
325-400	37	10.1
<400	0	7.2



Figure 1. Surface morphology of MAR M-200 particles at three magnifications.



Figure 2. Cross-section of particle showing dendritic structure.

in Figure 2. The dendritic structure existed throughout the whole cross-section of the particles. All particles exhibited the dendritic structure. Although Patterson et al³ reported that microcrystalline structure for the smaller particles (3% of the particles having 20 μm diameter or less) were microcrystalline, this was not observed here. The microcrystalline structure is obtained at a cooling rate higher than that which produces the microdendritic structure. Thus, one can infer that the cooling rate in the present batch of particles was not sufficient to induce the microcrystalline structure. This could be due to the very small fraction of particles having diameters less than 37 μm in the present investigation (see Table I). The explanation provided by Hirth¹⁶ for the difference in morphology is based on the undercooling. If solidification starts at a temperature such that the heat of solidification does not heat the interface to a temperature equal to the equilibrium solidus temperature, the microcrystalline structure results. Compositional homogeneity (no segregation) occurs, and a large number of micrograins (or microcrystallites) is formed. On the other hand, if the cooling rate is not high enough to produce this effect, a microdendritic structure is formed.

CONSOLIDATION TECHNIQUE

The consolidation was carried out in the assembly shown in Figure 3a. The powder is placed in a steel tube and pressed using a hand press, after the end plugs are inserted. The explosive totally surrounds the steel tube and is contained by a cardboard (or steel) tube. Detonation is initiated at the top by using a small booster charge (DuPont Datasheet, C-4) and a detonator to which Primacord (E-cord) is attached. The system is suspended over a water-recovery tank (Figure 3b), in which the water serves principally as a deceleration medium.

This technique to explosively consolidate powders was chosen because of the ease with which the experiments could be conducted and the small amount of tooling required. The design and dimensions of the system were taken from Lennon et al¹⁰ and Bhalla and Williams.¹⁶ Although this system is very limited with respect to the final shape and size of compact obtained, it was thought to be satisfactory in the exploratory investigation, in which the primary objective was to demonstrate the feasibility of shock-wave compaction of rapidly solidified powders. The variation of the ratio of the explosive mass to the tube mass (E_m/T_m) was the parameter used to attempt to obtain consolidation throughout the thickness of the material. Hand-pressed TNT was used in all but one event; C-4 was found to have too much power and brisance at the E_m/T_m ratio used. In another event, the cardboard tube was replaced by a steel tube to understand the role played by and possible benefit derived from the containment of the explosion. Table II shows the results obtained. By comparing trials T-1, T-2, T-3, and T-4, in which the mass of explosive (TNT) was kept constant, it can be seen that the reduction of the tube thickness has a clear effect on the compaction achieved. The experiment carried out using a mild steel cylinder in place of cardboard showed that the same compaction can be obtained at a lower E_m/T_m ratio, i.e., there are definite advantages in containing the explosion. Figure 4 shows, in graphical form, the information presented in Table II. Events T-5 and T-7 were not included, because of the additional parameters.

The wave propagation and wave interaction processes responsible for consolidation of the powders are not very well understood at this moment. Essentially, the detonation of the explosive, at a grazing incidence, accelerates the tube wall, and the tube wall transmits the shock wave to the powder. This wave attenuates itself rapidly as it travels inwards. Because the axisymmetric configuration of the shock wave, it converges along the longitudinal axis of the cylinder resulting in reinforcement. Figure 5 shows, schematically, the configuration for a strong initial shock pulse. The

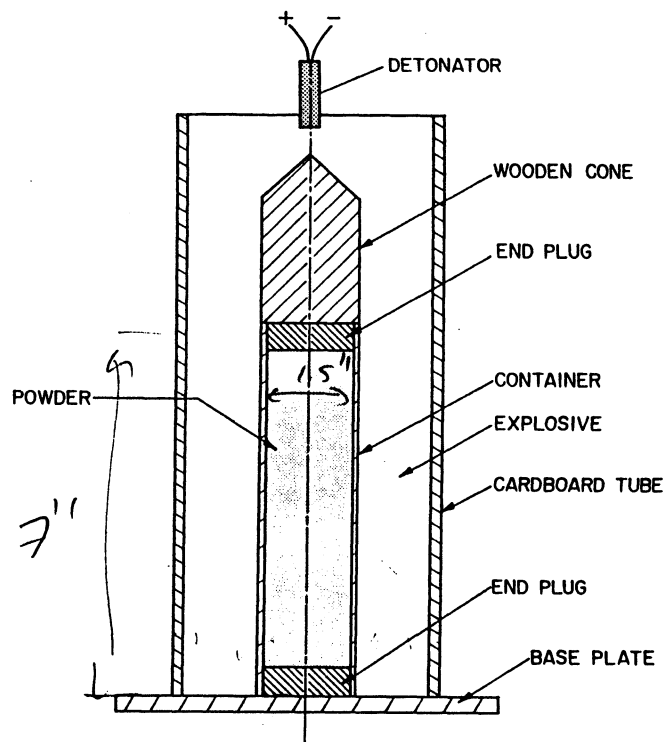
superposition of the waves at the center generates a second shock pulse, called a Mach wave. This Mach wave results in complete melting of the central core, with ejection of the molten material, when its amplitude is high enough. Therefore, the E_m/T_m ratio is very critical in this type of configuration: it should be high enough to produce full compaction and not high enough to allow the damaging effects of the Mach wave. Yust and Harris¹⁷ report the central melting observed in shock-consolidated alumina. In events T-6 and T-7, a small central hole (2 mm diameter) was formed, indicating that the E_m/T_m should be slightly reduced to obtain optimum compaction.

CHARACTERIZATION OF CONSOLIDATED POWDERS

The microstructural features at different values of E_m/T_m are shown in Figure 6. At the E_m/T_m ratio of 3.48, only the external layer of the compact consolidated. The particles (Figure 6a) show that the external layers underwent more deformation than the core. Small voids (black) can be seen, principally at triple junctions. Upon increasing the E_m/T_m ratio, a better interlocking between the particles can be seen. The flow of material can be observed by the distortion of the dendrites. The white regions are due to melting, as will be clear from the transmission electron microscopy results. As shown in the figure, the amount of interparticle melting increased with E_m/T_m ratio. These observations are in accord with Raybould's¹² recent results for AISI 304 L stainless steel.

As expected, the hardness increase after consolidation is significant. Figure 7 shows the microindentation hardness throughout the cross-section for two E_m/T_m ratios. The load used was 50 gram-force and the as-received hardness of the particles was 357 HV. The increase to 700 HV on consolidation is indicative of the great amount of substructural strengthening produced by the shock wave. This feature is thought to be a unique advantage of shock-wave consolidation over other techniques. Although the other mechanical properties have not been evaluated at this point, the high hardness indicates very favorable mechanical strength. For AISI 304 L stainless steel, Raybould¹² obtained a hardness of 420 HV and very favorable mechanical properties.

The deformation structures produced by shock-wave compaction are, in many ways, unique. Two substructurally different regions were clearly identified. This could be ascertained by electropolishing (with a Fischione twin-jet polisher) 3 mm discs punched from thin (0.2 mm) sawed slices for transmission electron microscopy (utilizing a Hitachi H.U. 200 F transmission electron microscope operated at 200 kV accelerating voltage). Figure 8a shows optical micrographs of the electron transparent region surrounding the electropolished hole in a typical specimen. Adjacent to the hole is a reasonably sized pool of solidified interparticle melting region, as well as regions that exhibit the dendritic structure (arrow in insert). Figure 8b shows the interface between these two regions (arrow in Figure 8a) by transmission electron microscopy. The boundary is quite well defined, and there is no similarity between the features of the two regions. They can be seen separately in the additional images and corresponding selected-area electron diffraction patterns shown in Figures 9a and 9b. The interparticle melt region can be described as microcrystalline (Figure 9b). The diffraction patterns for the microcrystalline regions in Figures 8b and 9b eloquently show the extremely small sizes of the grains; almost continuous rings can be seen. This microcrystalline morphology is undeniably associated with extremely high cooling rates; Raybould¹² estimates it to be around 10^6 K/s. In any case, it should be higher than the one originally undergone by the particles (10^4 - 10^5 K/s), because no segregation can be seen by either optical or transmission electron microscopy. These micrograins (less



▲ Figure 3a. Schematic of direct explosive system used.

▼ Figure 3b. System ready for explosive event.

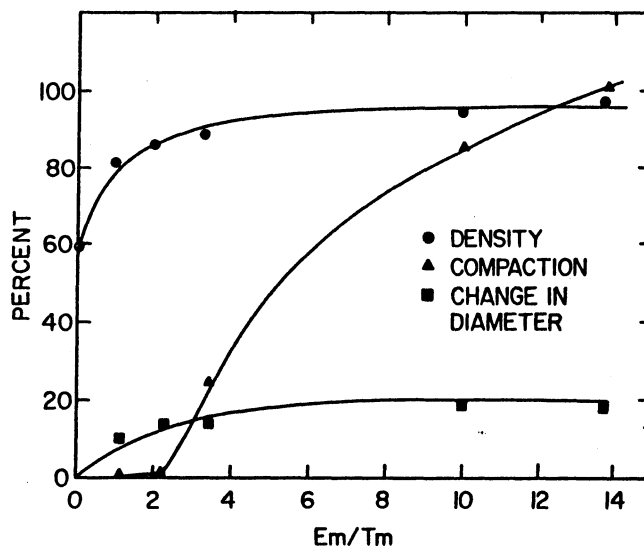
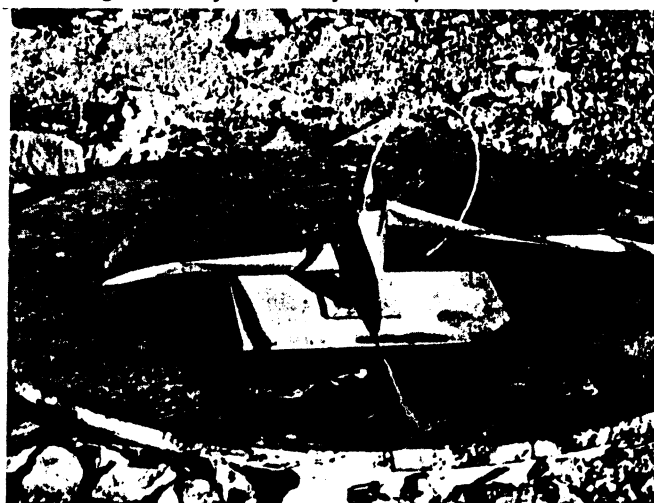


Figure 4. Effect of E_m/T_m (explosive mass/tube mass) ratio on density, compaction, and change in diameter of compact.

TABLE II
Effect of Explosive Mass-to-Container Mass Ratio (E_m/T_m) on Compaction of MAR M-200
Rapidly Solidified Powders Using Explosive TNT

Trial No.	Container Wall Thickness (mm)	Initial Packing Density (% of theoretical)	Explosive Packing Density (g/cm ³)	E_m/T_m	Compacted Density (% of theoretical)	Compaction (%)	Change in Container Diameter (%)
T-1	1.0	63	0.87	3.43	89.0	23.3	18
T-2	1.4	60	0.84	2.16	86.7	0	14
T-3	3.0	60	0.90	1.09	84.3	0	10
T-4	0.5	57	0.95	9.95	93.0	89.5	17
T-5*	0.9	60	1.60	9.22	87.0	—	—
T-6	0.5	61	1.06	13.78	93.7	100	17
T-7**	0.5	61	1.02	8.83	95.3	100	16

*Explosive C-4; compact obtained in small pieces.

**Cardboard cylinder was replaced by mild steel cylinder of same diameter.

than 0.3 μm in diameter) are somewhat elongated in Figure 9b due to the directionality of heat transfer. This is a commonly observed feature (in a much larger scale) of solidification. On the other hand, the banded substructure shown by the inside of the particles (Figure 9a) is typical of shock-loaded superalloys.¹⁹⁻²¹ These medium- and low-stacking fault energy fcc alloys exhibit this substructure after shock loading. These bands cannot be clearly distinguished, but seem to be a combination of stacking faults, dislocations, twin faults, and very thin twins. The diffraction pattern of Figure 9a shows the spots and streaking characteristic of fault reflections.

Although it is somewhat premature at this point to model the consolidation process, one can speculate on what is happening at the wave front. Figure 10 shows idealized spherical particles being traversed by a shock pulse. The *sine qua non* requirement for a shock wave is a state of uniaxial strain, i.e., no lateral flow of material. This condition is, obviously, not satisfied at the edges of the particles, where residual plastic deformation is necessary to produce material flow into the voids. Hence, the shock wave becomes a plastic wave in these regions, retaining its steep shock front only in the internal part of the particles. The conversion of the shock wave into a plastic wave is accompanied by a decrease in its velocity. This velocity has been estimated by von Karman and Duwez²² to be proportional to the square root of the work-hardening rate. The attendant degree of irreversibility of the process increases with dissipation of

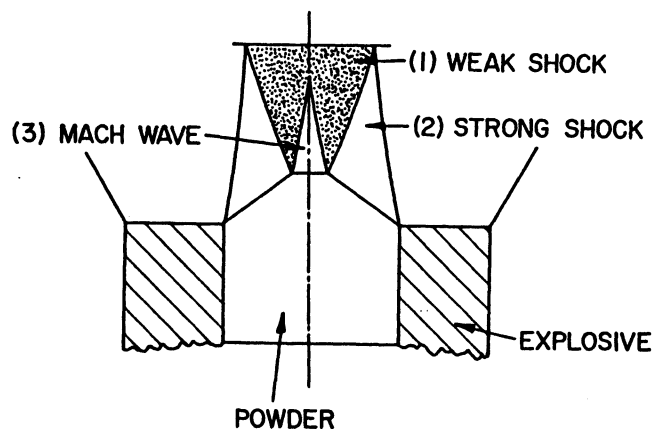


Figure 5. Configuration of shock pulses in direct explosive system when Mach wave is formed (Adapted from Staver¹⁶).

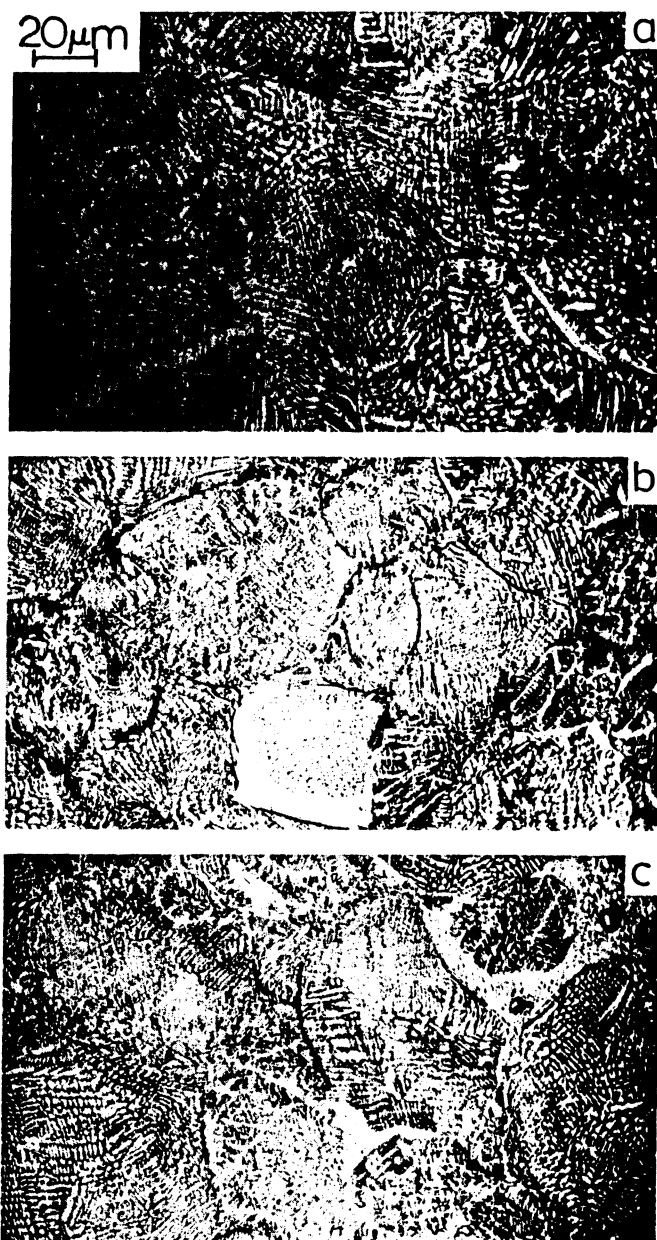


Figure 6. Microstructure of explosively consolidated powders at different E_m/T_m ratios (sections normal to tube axis) (a) 3.45; (b) 9.95; (c) 13.78.

the energy as heat. There are three sources of temperature rise: hydrodynamic temperature rise, plastic wave temperature rise (internal energy dissipation processes), and interparticle friction. The strains close to the interfaces are extremely high and lead, under adiabatic (or quasi-adiabatic) conditions, to temperature rises that can easily cause melting. This temperature rise is extremely localized and the high thermal conductivity of the metal causes ultra-high cooling rates, reminiscent of splat-cooling, in which the same principle of cooling operates. The plastic deformation is carried out in the wave-front region. The time can be estimated by taking the average plastic wave velocity as one-third of the shock-wave velocity and its average propagation distance as $20\text{ }\mu\text{m}$. The time is approximately $2 \times 10^{-2}\text{ }\mu\text{s}$, which is much lower than the initial pulse duration of the shock wave. Therefore, it can be assured initial wave front is followed by a shock wave traveling in the already solidified material. Wave reflection at the free-particle surfaces undoubtedly takes place and contributes to the process, but is not considered in this preliminary analysis. The results are exemplified in the deformation-induced microstructures evident in Figures 8b and 9a.

A great portion of the interparticle welds seems to be, under optical microscopy, a solid-state process. There should be interparticle melting even there; however, the layer is so thin that it cannot be seen. Since the cooling rate would be even higher in this case, it could be speculated that a very thin layer of amorphous or micrograin alloy is formed at these interfaces.

CONCLUSIONS

The following conclusions can be derived from the exploratory investigation whose results have just been described.

1. It was demonstrated that consolidation of MAR M-200 rapidly solidified powders by shock waves is a viable process.
2. A significant increase in hardness was obtained: the microindentation hardness increased from HV 357 to HV 700.
3. The bonding is produced by the heat generated by the quasi-adiabatic deformation taking place close to the interfaces.
4. The substructure is characterized by two distinct regions. The portion of the particles that remains solid exhibits a high density of defects in somewhat planar arrays, as would be expected after the passage of a shock wave. The interparticle melting regions, on the other hand, show the microcrystalline structure indicative of ultra-high cooling rates. It is thought that in the other interfacial regions a very thin layer of amorphous-like alloy is formed.

ACKNOWLEDGMENTS

The rapidly solidified MAR M-200 powder was kindly provided by Mr. A.R. Cox, of Pratt and Whitney Government Products Division (West Palm Beach, Florida). This research was partially supported by National Science Foundation Grant No. DMR-796102 and by the New Mexico Tech Research and Development Division; the help provided by Dr. M. Brook and Mr. L. Kempton is gratefully acknowledged.

References

1. R. Mehrabian, B.H. Kear, and M. Cohen, *Rapid Solidification Processing*, Claitor's Publishing Division, Baton Rouge, Louisiana, 1978.
2. *Proc. Second Intl. Conf. on Rapid Solidification Processing*, 1979, to be published.
3. R.J. Patterson II, A.R. Cox, and E.C. van Reuth, "Rapid Solidification Rate Processing and Application to Turbine Engine Materials," *J. of Metals* 32 (9) (September 1980) p. 34-39.
4. M. Cohen, B.H. Kear, and R. Mehrabian, *Proc. Second Intl. Conf. on Rapid Solidification Processing*, 1979, to be published.
5. J. Pearson, ASTM Creative Manufacturing Seminar, paper SP 60-158, 1980.
6. O. Roman, A.P. Bogdanov, I.M. Pickus, V.A. Korol and H.R. Luchenok, "Behavior of Fine Dispersed Powder Materials During Explosive Loading," *Proc. 6th Intl. Conf. on High Energy Rate Fabrication*, Aachen, Germany, 1977, p. 6.6.1-6.6.14.
7. O. Roman, and G. Gorobtaov, "Fundamentals of Explosive Compaction of Powders," *Shock Waves and High-Strain-Rate Phenomena in Metals: Concepts and Applications*, ed. by M.A. Meyers and L.E. Murr, Plenum Press, New York, 1981, p. 829-841.

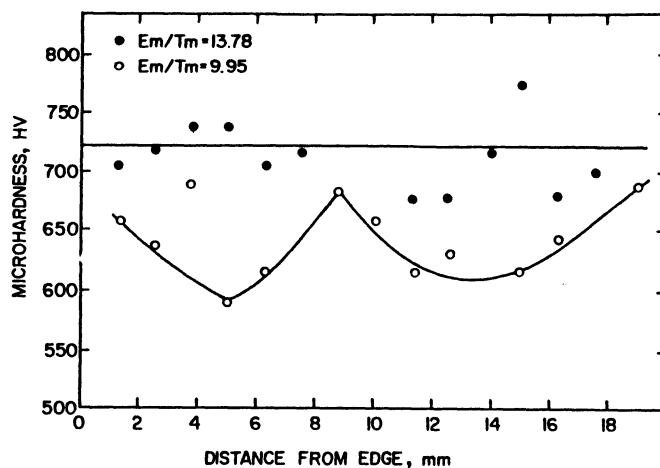


Figure 7. Variation of microindentation hardness along diameters (HV, 50 gram-force load).

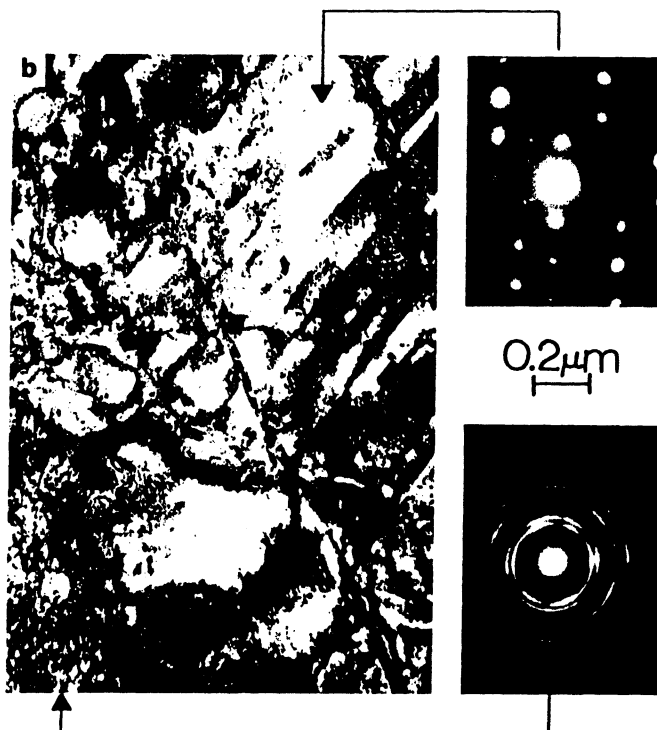
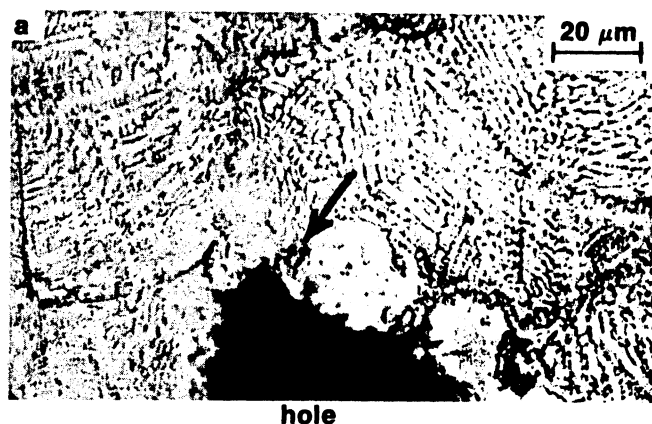


Figure 8a. Optical micrograph obtained by etching specimen used for transmission-electron microscopy showing interparticle melt region (arrow).

Figure 8b. Interface between interparticle melting region and particle.

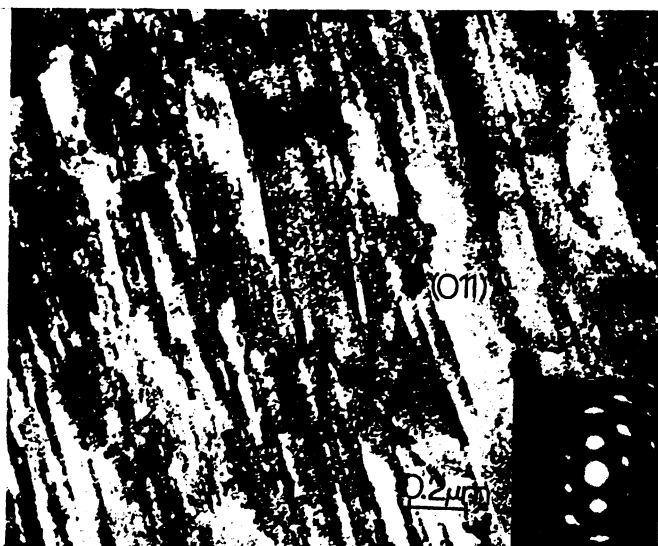


Figure 9a. Defect substructure characteristic of particle interiors.

Figure 9b. Microcrystalline structure characteristic of inter-particle melting region.

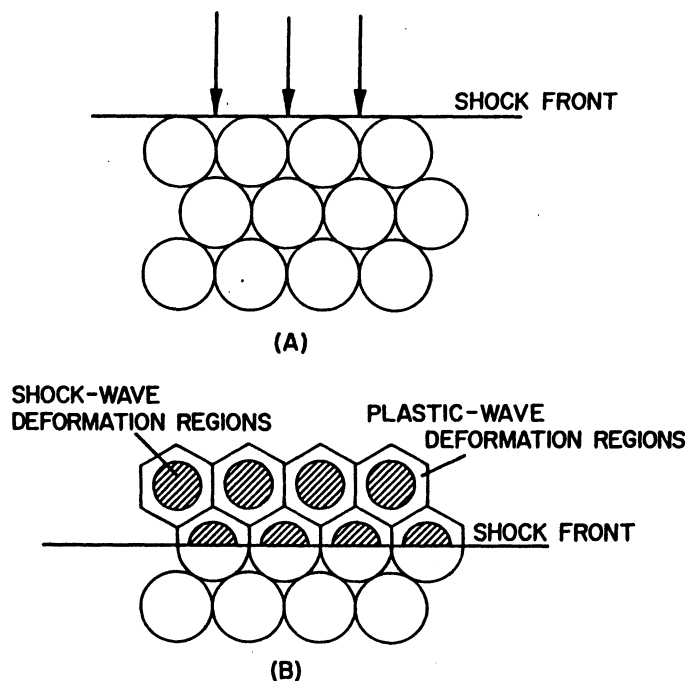


Figure 10. Schematic showing propagation of wave through powder and two distinct wave regimes.

8. A. Deribas, "Explosive Metal Working in the U.S.S.R.," *Shock Waves and High-Strain-Rate Phenomena in Metals: Concepts and Applications*, ed. by M.A. Meyers and L.E. Murr, Plenum Press, New York, 1981, p. 915-939.
9. G.S. Clyne, and W. Johnson, "The Dynamic Compaction of Powdered Materials," *Mat. Sci. and Eng.* 30 (1977) p. 121-139.
10. C.R.A. Lennon, A.K. Bhalla, and J.D. Williams, "Explosive Compaction of Metal Powders," *Powder Metallurgy* (1) (1978) p. 29-34.
11. D. Raybould, "The Production of Strong Parts and Non-Equilibrium Alloys by Dynamic Compaction," *Shock Waves and High-Strain-Rate Phenomena in Metals: Concepts and Applications*, ed. by M.A. Meyers and L.E. Murr, Plenum Press, New York, 1981, p. 896-911.
12. D. Raybould, "The Properties of Stainless Steel Compacted Dynamically to Produce Interparticle Welding," *J. Metals Sci.* 16 (1981) p. 589-598.
13. D. Raybould, D. Morris, and G.A. Cooper, "A New Powder Metallurgy Method," *J. Metals Sci.* 14 (1979) p. 2523-2528.
14. P.R. Holland, A.R. Cox, and R.J. Patterson II, "Rapid Solidification Effects on Alloy Structures," *Rapid Solidification Processing*, ed. by R. Mehrabian, B.H. Kear, and M. Cohen, Claitor's Publishing Division, Baton Rouge, Louisiana, 1978, p. 246-257.
15. J.P. Hirth, "Nucleation, Undercooling and Homogeneous Structures in Rapidly Solidified Powders," *Met. Trans.* 9A (1978) p. 401-404.
16. A.K. Bhalla, and J.D. Williams, "The Role of the Container in the Consolidation of Powders by Direct Explosive Compaction," *Proc. 8th Intl. Conf. on High Energy Rate Fabrication*, Univ. of Denver, Colorado, June 1975, p. 2.2.1-2.2.48.
17. C.S. Yust and L.A. Harris, "Observation of Dislocations and Twins in Explosively Compacted Alumina," *Shock Waves and High-Strain-Rate Phenomena in Metals*, ed. by M.A. Meyers and L.E. Murr, Plenum Press, New York, 1981, p. 881-894.
18. A.M. Staver, "Physical Phenomena at the Compression of Powder Materials by Explosives," *Proc. 8th Intl. Conf. on High-Energy-Rate Fabrication*, Univ. of Denver, Colorado, 1975, p. 2.1.1-2.1.31.
19. L.E. Murr, H.R. Vidyantath and J.V. Foltz, "Comparison of the Substructures and Properties of Nickel, TD-Ni, Chromel-A, Inconel 600 and TD-NiCr Following Explosive Shock Deformation," *Met. Trans.* 1A (1970) p. 3215-3223.
20. M.A. Meyers and R.N. Orava, "Thermomechanical Processing of Inconel 718 by Shock-Wave Deformation," *Met. Trans.* 7A (1976) p. 179-190.
21. R.N. Orava, "Response of Nickel-Base Superalloys to Thermomechanical Processing by Shock-Wave Deformation," D.R.I. - Univ. of Denver, Report No. DRI - 2638, U.S. Naval Air Systems Commands, April 1979.
22. T. von Karman and P. Duwez, "The Propagation of Plastic Deformation in Solids," *J. Appl. Phys.* 21 (1950) p. 987-994.

ABOUT THE AUTHORS



Marc A. Meyers is associate professor of metallurgy at New Mexico Institute of Mining and Technology. He was previously associated with South Dakota School of Mines and Technology and the Military Institute of Engineering (IME) in Rio de Janeiro, Brazil. Dr. Meyers received a diploma in Mechanical Engineering from the Federal University of Minas Gerais, Brazil, and MS and PhD in metallurgy from the University of Denver. He has published more than 40 scientific and technical articles and is the co-editor with Dr. L.E. Murr of the recent compendium *Shock Waves and High-Strain-Rate Phenomena in Metals: Concepts and Applications*. He is also the co-author of a book on mechanical metallurgy to be published in 1982. He is a member of The Metallurgical Society.



B. Bhushan Gupta is a research assistant in the Department of Metallurgical and Materials Engineering, New Mexico Institute of Mining and Technology, where he is currently pursuing a graduate degree. He holds a BSc in metallurgical engineering from the Regional Engineering College, Warangal, India and an MSc from Imperial College, London.



Lawrence E. Murr is vice president for Academic Affairs and Research and professor of Materials Science at the Oregon Graduate Center. He was formerly professor of Metallurgical and Materials Engineering and President of the New Mexico Tech Research Foundation at New Mexico Institute of Mining and Technology. He holds a BSc in Physical Science from Albright College and BSEE (electronics), MS in engineering mechanics, and PhD in solid-state science, all from the Pennsylvania State University. He is a member of The Metallurgical Society and is active as a consultant. He has published more than 325 journal articles and 8 books in areas ranging from solid-state electronics, interfacial phenomena, metal physics, metallurgy, and the mineral and materials sciences.